J. Am. Soc. Mass Spectrom. (2016) 27:1263–1276
DOI: 10.1007/s13361-016-1383-3

RESEARCH ARTICLE

Analysis of Bacterial Lipooligosaccharides by MALDI-TOF MS with Traveling Wave Ion Mobility

Nancy J. Phillips,[1] Constance M. John,[2,3] Gary A. Jarvis[2,3]

[1]Department of Pharmaceutical Chemistry, University of California, San Francisco, CA 94143, USA
[2]Center for Immunochemistry, Veterans Affairs Medical Center, 4150 Clement Street, San Francisco, CA 94121, USA
[3]Department of Laboratory Medicine, University of California, San Francisco, CA 94143, USA

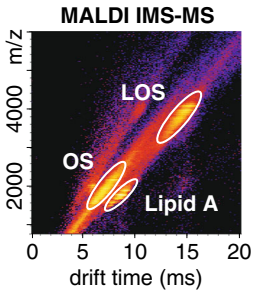

Abstract. Lipooligosaccharides (LOS) are major microbial virulence factors displayed on the outer membrane of rough-type Gram-negative bacteria. These amphipathic glycolipids are comprised of two domains, a core oligosaccharide linked to a lipid A moiety. Isolated LOS samples are generally heterogeneous mixtures of glycoforms, with structural variability in both domains. Traditionally, the oligosaccharide and lipid A components of LOS have been analyzed separately following mild acid hydrolysis, although important acid-labile moieties can be cleaved. Recently, an improved method was introduced for analysis of intact LOS by MALDI-TOF MS using a thin layer matrix composed of 2,4,6-trihydroxyacetophenone (THAP) and nitrocellulose. In addition to molecular ions, the spectra show in-source "prompt" fragments arising from regiospecific cleavage between the lipid A and oligosaccharide domains. Here, we demonstrate the use of traveling wave ion mobility spectrometry (TWIMS) for IMS-MS and IMS-MS/MS analyses of intact LOS from *Neisseria* spp. ionized by MALDI. Using IMS, the singly charged prompt fragments for the oligosaccharide and lipid A domains of LOS were readily separated into resolved ion plumes, permitting the extraction of specific subspectra, which led to increased confidence in assigning compositions and improved detection of less abundant ions. Moreover, IMS separation of precursor ions prior to collision-induced dissociation (CID) generated time-aligned, clean MS/MS spectra devoid of fragments from interfering species. Incorporating IMS into the profiling of intact LOS by MALDI-TOF MS exploits the unique domain structure of the molecule and offers a new means of extracting more detailed information from the analysis.

Keywords: Ion mobility spectrometry, Traveling wave ion mobility, IMS, TWIMS, IMS-MS, IMS-MS/MS, Lipooligosaccharides, Lipopolysaccharides, LOS, LPS

Received: 14 December 2015/Revised: 11 March 2016/Accepted: 12 March 2016/Published Online: 7 April 2016

Introduction

Structural elucidation of endotoxins, the complex glycolipids of the outer membrane of Gram-negative bacteria, presents a number of analytical challenges. The amphipathic nature and inherent heterogeneity of the isolated glycolipids, also known as lipooligosaccharides (LOS) or lipopolysaccharides (LPS), complicate chromatographic and structural studies. Nonetheless, detailed characterization of these surface-exposed antigens and microbial virulence factors is essential to understanding how they mediate bacterial survival and interact with the human immune system [1, 2].

In general, LOS are made by "rough" (R)-type bacteria that colonize mucosae of respiratory and genital surfaces [3], whereas LPS are made by "smooth" (S)-type bacteria, such as enteric organisms [4]. Both LOS and LPS contain a lipid A moiety that anchors the molecule into the lipid bilayer and a core oligosaccharide directly attached to the lipid A. LPS also contain strain-specific "*O*-antigen" polysaccharides not found in LOS. The lipid A moiety is commonly a conserved α1,6-linked diglucosamine structure bearing *N*- and *O*-linked fatty acid chains, whereas core oligosaccharide structures are much more variable in terms of size (typically ~ 8–12 sugars [4]), monosaccharide constituents, and branching patterns. The monosaccharide linking the core oligosaccharide to lipid A is typically 3-deoxy-D-*manno*-octulosonic acid (Kdo).

Nancy J. Phillips and Constance M. John contributed equally to this work.

Correspondence to: Gary A. Jarvis; *e-mail:* Gary.Jarvis@ucsf.edu

LOS isolates generally exhibit naturally occurring heterogeneity in both their core oligosaccharide and lipid A domains. While most commonly diphosphorylated, lipid A species can also be decorated with additional phosphate (P) and phosphoethanolamine (PEA) groups. Variability in fatty acid substituents on lipid A, as well as non-stoichiometric substitutions of *O*-linked moieties, such as sialic acid (*N*-acetylneuraminic acid, Neu5Ac), acetate, or glycine on the core oligosaccharide, increases LOS complexity.

Recognition of Gram-negative bacteria by the innate immune system involves binding of LOS or LPS with Toll-like receptor 4 (TLR4) on human cells, which induces inflammatory cytokines and engages host defense mechanisms [5]. Variation in structural features of the lipid A and oligosaccharide components of LOS can be correlated with differences in bioactivity [5]. A key determinant of toxicity and pathophysiology of infections with *Neisseria* spp. is the acylation state of lipid A [6, 7]. Modification of lipid A with PEA increases resistance of *N. gonorrhoeae* to complement killing and increases survival of both gonococci and meningococci in vivo [8]. We have shown that the degree of phosphorylation of lipid A of Neisserial LOS is correlated with its inflammatory potential [9–13] and appears to play a role in the immune privilege enjoyed by commensal *Neisseria* [12, 14].

The carbohydrate moieties of LOS are antigens presented on the bacterial cell surface that can interact with host proteins [15] and host glycans [16]. Some LOS carbohydrate moieties mimic human glycolipid and glycosphingolipid structures [17, 18]. Lacto-*N*-neotetraose (Galβ1→4GlcNAcβ1→3Galβ1→4Glc) expression is associated with greater ability of *N. gonorrhoeae* to infect men [19], and induces bactericidal IgG for L2, L3, L4, and L7 *N. meningitidis* immunotypes [20, 21]. Our data show that addition of Neu5Ac, acetate, and PEA to the oligosaccharide moieties of LOS impacts the pathophysiology of infection with *N. meningitidis* [13]. The expression of PEA, particularly on *O*-3 of HepII, or of Neu5Ac on the oligosaccharide of meningococcal LOS, inhibits complement activation [20–23].

Traditionally, to obtain the level of structural detail required for LOS structure/activity studies, the two domains of the molecule were analyzed separately following selective cleavage of the labile ketosidic linkage between the lipid A and the oligosaccharide moieties by mild acid hydrolysis [4, 24]. Alternatively, LOS can be *O*-deacylated to remove *O*-linked fatty acids from the lipid A, or fully *O*- and *N*-deacylated to generate "backbone" LOS [25, 26]. However, other acid-labile moieties, such as phosphate groups and Neu5Ac, can also be removed [10] and the release of biologically interesting *O*-linked moieties, such as acetate and glycine, occurs as an unwanted consequence of *O*-deacylation [27].

Very few groups have attempted structural analysis of intact LOS, with or without any preliminary chromatographic separation [24, 28–30]. Recently, an improved method was introduced for the analysis of intact LOS by negative-ion, matrix-assisted laser desorption/ionization time-of-flight mass spectrometry (MALDI-TOF MS) that utilizes a thin layer matrix composed of 2,4,6-trihydroxyacetophenone (THAP) and nitrocellulose [31]. We and others have exploited this methodology to profile complex LOS mixtures without any chemical modifications [9, 10, 30, 32]. In the MS analysis, LOS molecular ions readily undergo "prompt" fragmentation, a type of in-source decay occurring at the sample surface in a few picoseconds to nanoseconds before or during desorption [33], to give fragments arising from the oligosaccharide and lipid A domains of the molecule through cleavage at the labile ketosidic linkage [31, 34]. Prompt fragments representing both domains of the molecule corroborate proposed compositions of the LOS molecular ions detected. Although previously only conducted in linear mode, analysis of intact LOS by high-resolution, reflectron mode MALDI-TOF MS has now been achieved [12, 13, 32, 35]. The ability to measure monoisotopic molecular ions with good mass accuracy (<20 ppm) has dramatically improved the quality of the information that can be obtained from MALDI-TOF MS analysis of intact LOS.

Here, we introduce the application of ion mobility spectrometry (IMS), coupled with mass spectrometry (IMS-MS) and tandem mass spectrometry (IMS-MS/MS) [36], to further enhance the profiling and analysis of intact LOS at high resolution. In this work, we utilized a Synapt G2 HDMS equipped to perform traveling wave ion mobility spectrometry (TWIMS) in which ions are separated on the basis of their mobility through a stacked ring ion guide where a transient DC voltage is propagated in waves through the device in the presence of a drift gas [37, 38]. With IMS-MS experiments, ions are separated by size, shape, and charge. In complex samples, ions are resolved in plumes along "trend lines" according to chemical class due to differing size to mass ratios [39]. When plotted as mobility to mass, the average slope of the correlation lines fitted to the ion clusters increases in this approximate order: small molecules<oligonucleotides<carbohydrates<peptides <proteins<lipids [39–41]. Thus, for singly charged ions of the same nominal mass, lipids will generally have the slowest arrival time distribution in IMS, preceded by the other chemical classes.

The new approach to analysis of intact LOS that we present here takes advantage of the class-specific resolution of ions by IMS-MS. We demonstrate that the oligosaccharide and lipid A prompt fragments of LOS can be readily separated by IMS-MS into distinct ion plumes and highlight the advantages of this gas-phase separation for IMS-MS/MS analysis of precursor ions.

Experimental

Bacterial Strains and LOS Preparation

N. meningitidis serogroup C strain 89I is a clinical isolate that has been described previously [9, 10, 42]. *N. meningitidis* serogroup B strain 701 is an isolate from a throat culture of a carrier of *N. meningitidis* without disease obtained during a serogroup B vaccination trial in Norway. We recently

characterized the LOS from a large sampling of invasive and carrier strains of *N. meningitidis* from this study in order to correlate clinical outcomes with LOS structural features [13]. *N. flavescens* strain 4322 was available in the Center for Immunochemistry from the collection of the late Herman Schneider, formerly of the Walter Reed Army Institute of Research, and has been described previously [12]. LOS from all strains was extracted and purified by a modification of the hot phenol-water method [43, 44].

SDS-PAGE Analysis of Intact LOS

LOS samples were suspended (0.1 μg/μL) in Laemmli sample buffer (Bio-Rad, Hercules, CA, USA) with 2.5% (v/v) 2-mercaptoethanol (Sigma-Aldrich, St. Louis, MO, USA), and 10-μL aliquots were separated by SDS-PAGE through a mini-Protean TGX precast 4%–20% gradient gel (Bio-Rad). Electrophoresed LOS molecules were visualized by silver stain [43].

Preparation of Intact LOS for Analysis by MALDI-TOF MS

As we have previously reported [9, 10, 12, 13], intact LOS was deposited on top of a prespotted matrix layer for MALDI-TOF MS analysis. The matrix solution was prepared by mixing a solution of THAP (200 mg/mL in methanol; Sigma-Aldrich) with a solution of nitrocellulose transblot membrane (15 mg/mL in acetone/isopropanol, 1:1; Bio-Rad) in a 3:1 (v/v) ratio. This slight modification of the original published protocol [31] produced thicker matrix layers optimized for analysis on the Synapt G2 HDMS (described below). Aliquots of the matrix solution (~1 μL) were spotted within inscribed circles on a stainless steel sample plate and allowed to air dry. Meanwhile, intact LOS (4 to 10 mg/mL) was suspended in a solution of methanol/water, 1:3, containing 5 mM EDTA, and an aliquot was desalted with a few cation exchange beads (Dowex 50WX8-200) that had been converted to the ammonium form. The desalted LOS solutions were then mixed 9:1 (v/v) with 100 mM dibasic ammonium citrate, and ~1 μL aliquots of this final solution were deposited on the dried matrix spots and allowed to air dry. For the LOS of ~4000 MW examined in this study, this amounted to ~1–2.5 nmol loaded per spot.

Negative-Ion MALDI-TOF MS and MS/MS Analyses of Intact LOS

MALDI-TOF MS was performed on a Synapt G2 high definition mass spectrometer (HDMS) (Waters Corporation, Manchester, UK) with an orthogonal TOF mass analyzer in "sensitivity mode." The instrument is equipped with a Nd:YAG laser operated at a wavelength of 355 nm, with a 200 Hz firing rate. In general, spectra were acquired for ~1 min, with a scan duration of 1.0 s and an overall cycle time of 1.024 s. Spectra were digitally smoothed and baseline-corrected using MassLynx 4.1 software. The instrument was calibrated using the mass for the monoisotopic $(M–H)^-$ ions for bovine insulin at *m/z* 5728.5931, insulin B-chain at *m/z* 3492.6357, renin substrate at *m/z* 1756.9175, and angiotensin II at *m/z* 1044.5267 (all from Sigma-Aldrich).

For MS/MS analysis, precursor ions were typically selected with instrument LM and HM resolution settings of 4.7 and 15.0, respectively. In TOF MS/MS mode, fragmentation was achieved by applying collision energy in the Trap region of the T-wave ion mobility cell present in the Synapt G2 HDMS, with argon as collision gas. Trap collision energies of 85–110 V were required for optimum fragmentation of intact LOS $(M–H)^-$ ions.

Negative-Ion IMS-MS and IMS-MS/MS Analyses of Intact LOS

Ion mobility separations were performed on a Synapt G2 HDMS equipped with a T-wave ion mobility cell (Triwave) [37, 38], operating in MALDI mode. The T-wave device consists of three cells; a Trap cell, IMS cell, and Transfer cell. For IMS-MS experiments, the T-wave peak height voltage was 40 V and the T-wave velocity used was generally a variable wave velocity of 650 to 250 m/s. Typically, the T-wave mobility cell contained nitrogen at a pressure of ~2 mbar, trap gas flow was 0.4 mL/min, helium cell gas flow was 180 mL/min, IMS gas flow was 90 mL/min, and trap DC bias was 80 V. In IMS mode, spectra were typically acquired for 1–2 min, with scanning parameters as noted above.

For IMS-MS/MS experiments, collision energy was applied in the Transfer cell following IMS separation, at values ranging from 50 to 90 V, depending on the analyte. The Transfer cell contained argon as the collision gas. For analysis of oligosaccharide and lipid A prompt fragments, a T-wave variable wave velocity of 1100 to 200 m/s was used. Two-dimensional IMS spectra were viewed using DriftScope 2.1 software, and selected spectral regions were exported to MassLynx with retention of drift time information for generation of mobilograms and subspectra.

Results and Discussion

Molecular Weight Profiling of Intact LOS

Using a thin-layer matrix composed of THAP and nitrocellulose [31], intact LOS can be analyzed by MALDI MS, generally in the negative-ion mode [9, 10, 12, 13, 30–32, 35]. This method produces an envelope of $(M–H)^-$ ions, as well as informative prompt fragments arising from the lipid A and oligosaccharide domains of the molecule. An important benefit of the MALDI method is that predominantly singly charged ions are formed, which dramatically simplifies interpretation of the spectra of intact LOS. Within a spectrum, the masses for oligosaccharide and lipid A prompt fragments (assigned as B- and Y-type ions, respectively, according to the nomenclature of Domon and Costello [45]) derived from the same LOS species can be readily added together to confirm the composition of the corresponding $(M–H)^-$ ions for intact LOS. At high resolution, interpretation is aided by the fact that oligosaccharide and lipid

A prompt fragments can often be distinguished by their mass defect. Thus, in addition to molecular weight profiling, specific information about the overall architecture of LOS molecules is also obtained by MALDI MS.

Figure 1 shows plots of the high-resolution, negative-ion MALDI spectra of the LOS from three strains of *Neisseria*: *N. meningitidis* 89I, *N. meningitidis* 701, and *N. flavescens* 4322. The two strains of *N. meningitidis*

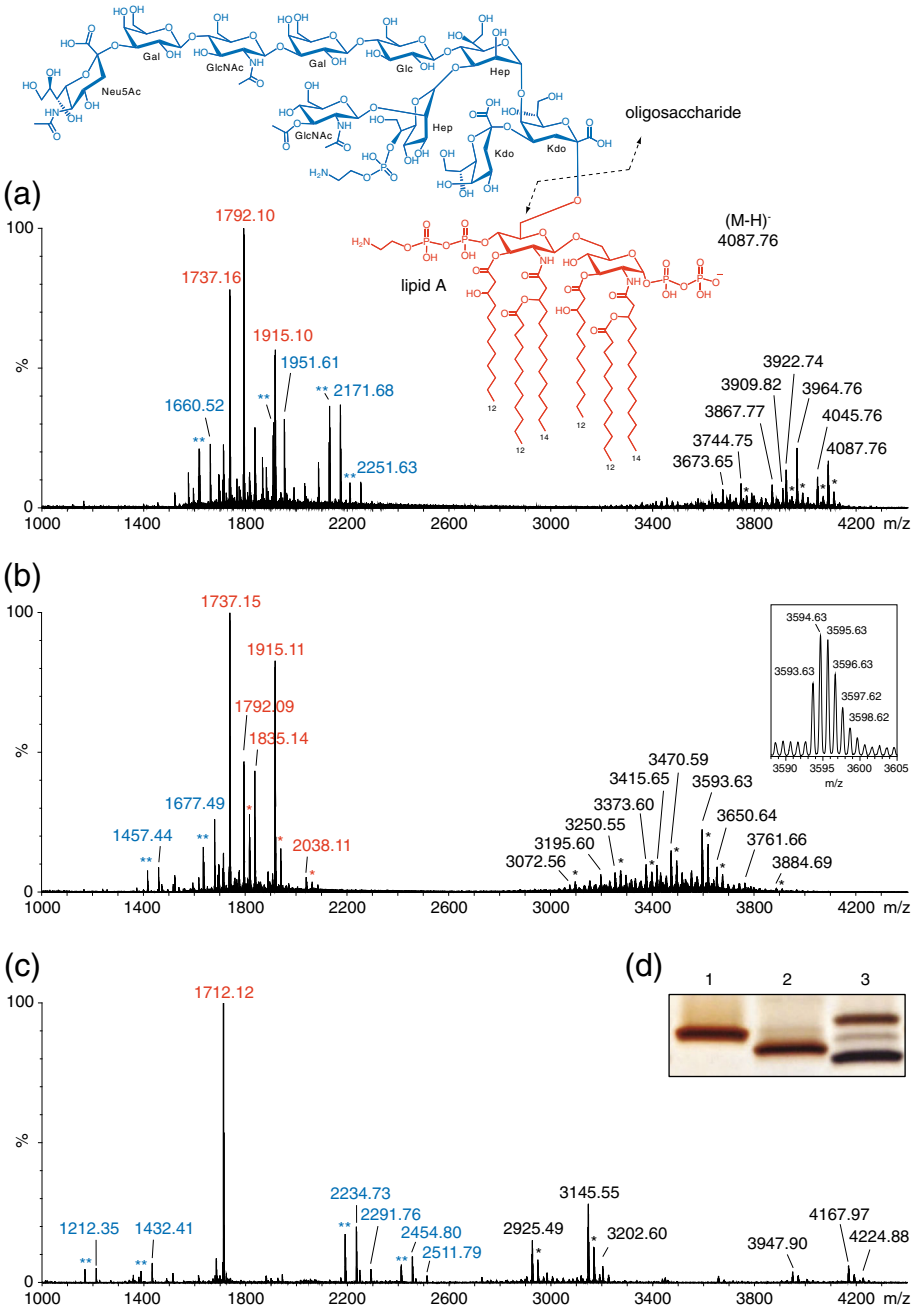

Figure 1. High-resolution, negative-ion MALDI-TOF MS of the intact LOS from *N. meningitidis* strains 89I **(a)**, *N. meningitidis* strain 701 **(b)**, and *N. flavescens* strain 4322 **(c)**. Deprotonated molecular ions, $(M–H)^-$, are labeled in black font, lipid A prompt fragments in red font, and oligosaccharide prompt fragments in blue font. Sodiated species are marked with a single asterisk, and decarboxylated oligosaccharide prompt fragments ($–CO_2$, –44 Da) are marked with two asterisks. The inset in panel **(b)** shows an expanded view of the resolved isotope peaks for the species at *m/z* 3593.63. The proposed structure for the species at *m/z* 4087.76 from *N. meningitidis* 89I LOS is shown above panel **(a)**. This is a prototypical Neisserial LOS structure bearing a hexaacylated lipid A and a decasaccharide moiety, the composition, sequence, and branching pattern of which have been previously reported [42, 50]. Both domains bear secondary modifications, including phosphates, phosphoethanolamines, and acetate groups. The dashed line with two arrowheads indicates the labile ketosidic linkage between the two domains. SDS-PAGE analysis of the three LOS preparations is shown in panel **(d)**: lane 1, *N. meningitidis* 89I; lane 2, *N. meningitidis* 701; and lane 3, *N. flavescens* 4322

(Figure 1a and b) show similar profiles, with $(M–H)^-$ ions in the *m/z* 3000 to 4300 range and prompt fragments in the *m/z* 1400 to 2300 range. Complexity in the molecular ion regions can be attributed to common features of Neisserial LOS, including heterogeneity in phosphate substituents on both the lipid A and oligosaccharide moieties, non-stoichiometric substitution with moieties such as acetate and glycine, and the presence of labile Kdo and Neu5Ac sugars that can be partially lost due to prompt fragmentation. Likewise, this complexity is represented in the lipid A and oligosaccharide prompt fragments as well (including further oligosaccharide fragments arising from gas-phase decarboxylation of Kdo-containing oligosaccharides). The lipid A moiety of Neisserial LOS can be variously phosphorylated with up to three P and two PEA moieties, whereas the prototypical oligosaccharide structure may or may not contain one PEA moiety [9, 10]. Previously we showed that the relative abundance of lipid A phosphoforms could be correlated with inflammatory potential of Neisserial LOS, with the more highly phosphorylated structures being more highly inflammatory [9, 10, 12]. Our recent work with a large group of carrier and disease-causing strains of *N. meningitidis* showed that lipid A phosphorylation states can also be correlated with clinical outcomes [13]. The inset above Figure 1a shows a proposed structure for the major LOS species at *m/z* 4087.76 in *N. meningitidis* 89I that represents a prototypical Neisserial LOS structure [9, 46–48]. The detailed lipid A and oligosaccharide structures depicted for the *N. meningitidis* 89I LOS, an L4 immunotype [49], are based on MS and NMR studies of the conserved Neisserial lipid A [50] and the L4 oligosaccharide [42]. Proposed compositions for all of the major $(M–H)^-$ ions and prompt fragments seen in the LOS from *N. meningitidis* strains 89I and 701 are given in Table 1, consistent with our previous reports on Neisserial LOS [9, 10, 13].

In contrast to the LOS from pathogenic *N. meningitidis*, the *N. flavescens* 4322 LOS shows one major lipid A prompt fragment at *m/z* 1712.12, corresponding to a diphosphorylated lipid A structure (Figure 1c). Previously we found that commensal strains of *Neisseria*, such as *N. flavescens*, do not express highly phosphorylated lipid A structures, and this is associated with reduced inflammatory potential of the LOS [12]. Although expressing only one lipid A phosphoform, the *N. flavescens* LOS sample is unusual in that it produces an extended range of putative molecular ion peaks and two groups of oligosaccharide prompt fragments. Analysis of the LOS from the three strains of *Neisseria* by SDS-PAGE (Figure 1d) revealed differences in the LOS banding patterns that were consistent with the MALDI spectra. Specifically, when run on a 4%–20% gradient SDS-PAGE gel, the two *N. meningitidis* strains each showed a single, major LOS band, whereas the *N. flavescens* LOS showed two widely separated major bands migrating above and below the *N. meningitidis* LOS species. A large gap in LOS banding patterns may signify a core LOS structure plus a semi-rough (SR)-type LPS form containing only one *O*-antigen repeat unit [4]. This possibility was further explored as discussed below.

Analysis of Intact LOS Using IMS-MS

As shown in Figure 1, the lipid A and oligosaccharide prompt fragments produced during MALDI MS analysis of intact LOS can occur in an overlapping mass range when they are similar in size [30]. When dealing with unknown LOS molecules, this situation has the potential to be confusing. Furthermore, clean selection of peaks for MS/MS analysis can be problematic if overlapping species differ by only a few Daltons.

The use of MALDI MS coupled with IMS circumvents these problems in an elegant fashion. Separation of ions in the IMS cell is dependent on molecular size, shape, and charge. Thus, IMS-MS spectra are essentially two-dimensional datasets containing *m/z*, drift time, and ion intensity information. Using traveling wave IMS on a Synapt G2 HDMS operating in negative-ion MALDI mode, we were able to resolve the oligosaccharide and lipid A prompt fragments into two distinct plumes of ions, as shown for the intact LOS from *N. meningitidis* 701 in Figure 2. The DriftScope image (Figure 2a) shows the carbohydrate ion plume cleanly preceding the lipid A ion plume, meaning that for species of comparable size, carbohydrate ions have smaller cross-sectional areas than lipid A ions do, allowing them to travel through the IMS cell faster. This finding is consistent with previous empirical observations of the relative ion mobilities of lipid and carbohydrate ions [39, 40]. The difference in relative size between these chemical classes may be attributed to their gas-phase packing efficiencies, which are dependent on forces such as van der Waals interactions, hydrogen bonding, and π–π interactions [39, 40]. Interestingly, although obviously identifiable because of their size, the $(M–H)^-$ ions for intact LOS occur in an ion plume drifting between the plumes for the two fragment types (Figure 2a), consistent with their hybrid structures. In addition to fully resolving all LOS-derived ions, the IMS-MS spectrum also shows the separation of minor amounts of contaminating species traveling ahead of the oligosaccharide ion plume. This general region also contains low abundance, doubly charged ions arising from the LOS glycoforms.

Using the DriftScope software, we selected regions from the two-dimensional plot for export to the Waters MassLynx program as indicated on Figure 2a. Three ion mobilograms generated from the chosen regions are shown in Figure 2b, and the associated mass spectra are shown in Figure 2c–e. The three subspectra are given on the same *m/z* scale for ease of comparison to the full MALDI spectrum shown in Figure 1b. The separation afforded by IMS cleanly resolves oligosaccharide and lipid A fragment ions into two populations.

In the case of *N. meningitidis* 89I LOS, where fragment ion overlap is more severe (Figure 1a), IMS nicely resolved the lipid A fragment ions at *m/z* 1792.10 and 1835.17 from the closely occurring oligosaccharide fragment ions at *m/z* 1794.61

Table 1. Masses and Proposed Compositions for the Molecular Ions and Lipid A and Oligosaccharide Prompt Fragments from *N. meningitidis* LOS

Strain	*m/z*	Derived composition[a]	Calc *m/z*	Δ PPM
89I	4087.756	TPLA PEA; 2 Kdo, 2 Hep, 3 Hex, 2 HexNAc, PEA, OAc, Neu5Ac	4087.768	-2.9
	4045.758	TPLA PEA; 2 Kdo, 2 Hep, 3 Hex, 2 HexNAc, PEA, Neu5Ac	4045.757	0.2
	3964.756	TPLA; 2 Kdo, 2 Hep, 3 Hex, 2 HexNAc, PEA, OAc, Neu5Ac	3964.759	-0.8
	3922.738	TPLA; 2 Kdo, 2 Hep, 3 Hex, 2 HexNAc, PEA, Neu5Ac	3922.749	-2.7
	3909.823	TPLA PEA - ($H_4P_2O_7$); 2 Kdo, 2 Hep, 3 Hex, 2 HexNAc, PEA, OAc, Neu5Ac	3909.824	-0.4
	3867.770	TPLA PEA - ($H_4P_2O_7$); 2 Kdo, 2 Hep, 3 Hex, 2 HexNAc, PEA, Neu5Ac	3867.814	-11.3
	3796.675	TPLA PEA; 2 Kdo, 2 Hep, 3 Hex, 2 HexNAc, PEA, OAc	3796.672	0.7
	3744.745	TPLA; 1 Kdo, 2 Hep, 3 Hex, 2 HexNAc, PEA, OAc, Neu5Ac	3744.701	11.8
	3673.654	TPLA; 2 Kdo, 2 Hep, 3 Hex, 2 HexNAc, PEA, OAc	3673.664	-2.6
	3453.617	TPLA; 1 Kdo, 2 Hep, 3 Hex, 2 HexNAc, PEA, OAc	3453.605	3.4
	2251.630	2 Kdo, 2 Hep, 3 Hex, 2 HexNAc, PEA, P, OAc, Neu5Ac	2251.634	-1.6
	2171.679	2 Kdo, 2 Hep, 3 Hex, 2 HexNAc, PEA, OAc, Neu5Ac	2171.667	5.4
	2031.587	1 Kdo, 2 Hep, 3 Hex, 2 HexNAc, PEA, P, OAc, Neu5Ac	2031.575	5.7
	1951.613	1 Kdo, 2 Hep, 3 Hex, 2 HexNAc, PEA, OAc, Neu5Ac	1951.609	2.1
	1880.591	2 Kdo, 2 Hep, 3 Hex, 2 HexNAc, PEA, OAc	1880.572	10.2
	1660.515	1 Kdo, 2 Hep, 3 Hex, 2 HexNAc, PEA, OAc	1660.514	0.9
	1915.103	TPLA PEA	1915.093	5.5
	1835.131	DPLA PEA	1835.126	2.6
	1792.101	TPLA	1792.084	9.5
	1737.159	TPLA PEA - ($H_4P_2O_7$)	1737.149	5.6
	1712.120	DPLA	1712.118	1.4
701	3884.687	TPLA PEA; 2 Kdo, 2 Hep, 3 Hex, HexNAc, PEA, OAc, Neu5Ac	3884.688	-0.3
	3761.662	TPLA; 2 Kdo, 2 Hep, 3 Hex, HexNAc, PEA, OAc, Neu5Ac	3761.680	-4.7
	3650.644	TPLA PEA; 2 Kdo, 2 Hep, 3 Hex, HexNAc, PEA, OAc, Gly	3650.614	8.1
	3593.630	TPLA PEA; 2 Kdo, 2 Hep, 3 Hex, HexNAc, PEA, OAc	3593.593	10.3
	3470.590	TPLA; 2 Kdo, 2 Hep, 3 Hex, HexNAc, PEA, OAc	3470.584	1.6
	3415.646	TPLA PEA - ($H_4P_2O_7$); 2 Kdo, 2 Hep, 3 Hex, HexNAc, PEA, OAc	3415.650	-1.1
	3373.599	TPLA PEA - ($H_4P_2O_7$); 2 Kdo, 2 Hep, 3 Hex, HexNAc, PEA	3373.639	-11.9
	3250.546	TPLA; 1 Kdo, 2 Hep, 3 Hex, HexNAc, PEA, OAc	3250.526	6.1
	3195.595	TPLA PEA - ($H_4P_2O_7$); 1 Kdo, 2 Hep, 3 Hex, HexNAc, PEA, OAc	3195.591	1.1
	3072.559	TPLA PEA - ($H_4P_2O_7$); 1 Kdo, 2 Hep, 3 Hex, HexNAc, OAc	3072.583	-7.7
	1968.572	2 Kdo, 2 Hep, 3 Hex, HexNAc, PEA, OAc, Neu5Ac	1968.588	-8.1
	1677.493	2 Kdo, 2 Hep, 3 Hex, HexNAc, PEA, OAc	1677.493	0.3
	1457.435	1 Kdo, 2 Hep, 3 Hex, HexNAc, PEA, OAc	1457.434	0.5
	2038.114	TPLA 2PEA	2038.101	6.3
	1915.108	TPLA PEA	1915.093	8.1
	1835.137	DPLA PEA	1835.126	5.9
	1792.089	TPLA	1792.084	2.8
	1737.147	TPLA PEA - ($H_4P_2O_7$)	1737.149	-1.3
	1712.127	DPLA	1712.118	5.4

[a]Abbreviations for LOS structural moieties: TPLA = triphosphorylated lipid A; DPLA = diphosphorylated lipid A; Kdo = 3-deoxy-D-*manno*-octulosonic acid; Hep = heptose; Hex = hexose; HexNAc = *N*-acetylhexosamine; P = phosphate; PEA = phosphoethanolamine; OAc = *O*-linked acetate; Gly = *O*-linked glycine; Neu5Ac = *N*-acetylneuraminic acid.

and 1836.61, respectively (Figure 3). Interestingly, in this high-resolution spectrum, fragment ions that are consistent with the presence of a phosphate group on the oligosaccharide (+80 Da) were readily apparent at *m/z* 2251.66, 2031.60, and 1740.52. Although phosphorylation of the oligosaccharide of LOS from several other genera such as *Campylobacter* [51] has been shown, we are the first to report phosphorylation of the oligosaccharide from *N. meningitidis* LOS [13], which was not detected in our previous analysis of the intact LOS by low resolution MALDI [9]. Here, the detection of the relatively minor peaks was facilitated by IMS and the high resolution of the analyses.

IMS-MS/MS for Generation of Clean Fragmentation Spectra

The separation (drift time difference) between oligosaccharide and lipid A prompt fragments afforded by IMS suggested that conducting MS/MS analysis of selected ions following IMS would be beneficial. Accordingly, we conducted CID in the Transfer region of the T-wave cell on the Synapt G2 HDMS with argon as the collision gas. Figure 4 shows the results obtained when the lipid A prompt fragment at *m/z* 1792.1 from *N. meningitidis* 89I LOS was selected for IMS-MS/MS. The DriftScope image (Figure 4b) is shown beneath the total ion mobilogram (Figure 4a). Here, we see that this method gives fragment ions that are time-aligned with their well-resolved precursor ions. The two regions outlined in white boxes were selected, and after export to MassLynx, the MS/MS spectra obtained are shown in Figure 4c and d. Figure 4d shows an extremely clean MS/MS spectrum of the triphosphorylated lipid A species, devoid of any extraneous peaks arising from the resolved oligosaccharide species, the MS/MS spectrum of which is shown in Figure 4c.

The MS/MS spectrum of the triphosphorylated lipid A species (Figure 4d) contains fragments arising from losses of

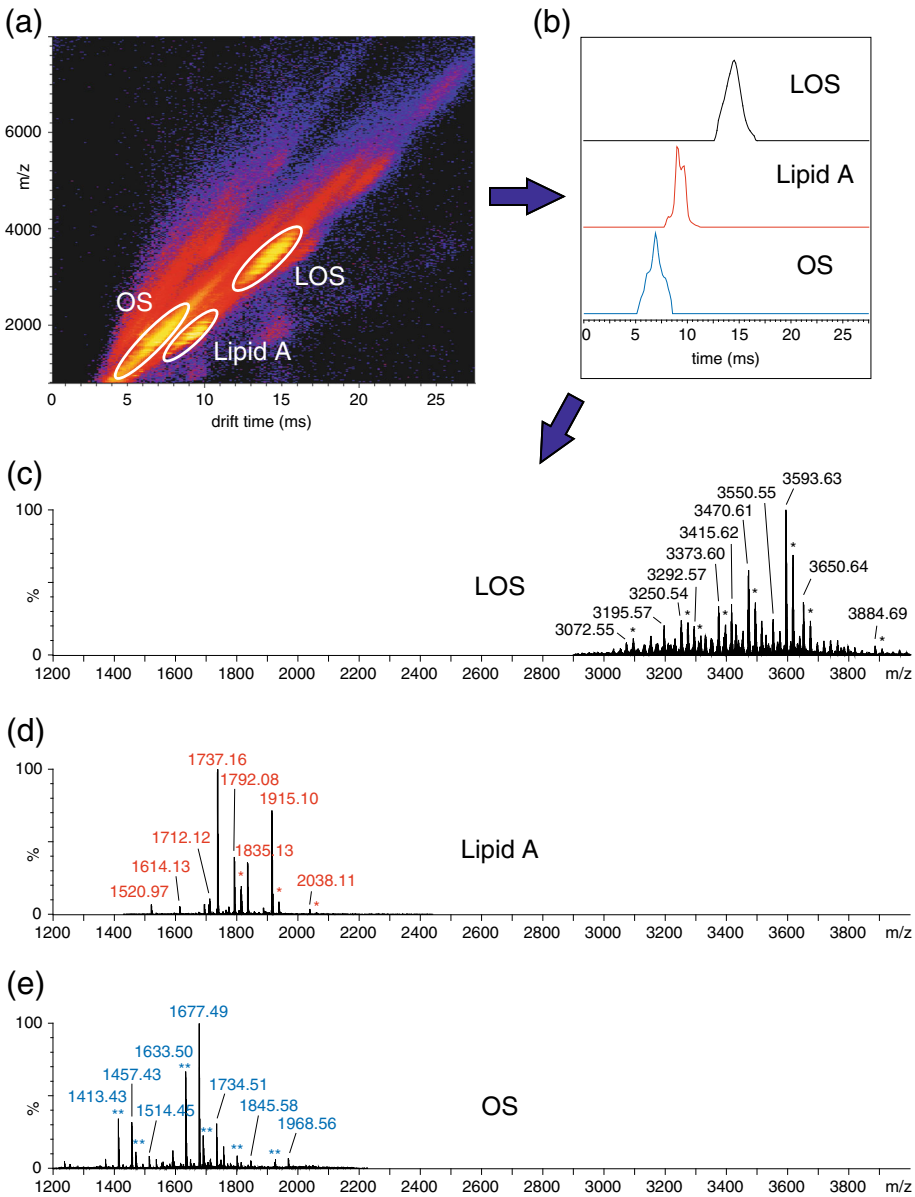

Figure 2. Analysis of the intact LOS from *N. meningitidis* 701 by MALDI-TOF MS with IMS. Panel **(a)** shows a two-dimensional plot of the IMS dataset (DriftScope heat map image). The LOS $(M–H)^-$ ions and oligosaccharide (OS) and lipid A prompt fragments occur in resolved ion plumes, as indicated on the plot. The three circled regions were selected and the data exported to MassLynx, with retention of drift time. Panel **(b)** shows the corresponding mobilograms viewed in MassLynx. The mass spectra for the extracted LOS $(M–H)^-$ ions, lipid A prompt fragments, and OS prompt fragments are shown in panels **(c)**, **(d)**, and **(e)**, respectively. Sodiated species are marked with a single asterisk, and decarboxylated oligosaccharide prompt fragments ($–CO_2$, –44 Da) are marked with two asterisks

fatty acids and phosphate moieties, from glycosidic bond cleavages, and from multiple bond cleavages. Ions at *m/z* 1712.19 and 1694.16 arise from loss of a single phosphate group from the precursor ion, whereas ions at *m/z* 1614.17 and 1596.16 result from loss of two phosphate groups. The ions at *m/z* 1477.98 and 1398.02 can be attributed to the concomitant loss of an *O*-linked C12:0 3-OH fatty acid plus P or 2P, respectively.

Fragment ions arising from the released phosphate moieties themselves are found in the low mass region of the spectrum and are diagnostic for the phosphoforms found on the structure [52]. As shown in Figure 4d, the major peaks at *m/z* 158.93 and 176.94 arise from pyrophosphate anions $(HP_2O_6)^-$ and $(H_3P_2O_7)^-$, respectively. Also present in the MS/MS spectrum are less abundant ions at *m/z* 238.89 and 256.91 that correspond to the triphosphate anions $(H_2P_3O_9)^-$ and $(H_4P_3O_{10})^-$, respectively. This latter pair of ions provides evidence for heterogeneity in the phosphoforms of the lipid A precursor ion at *m/z* 1792.14.

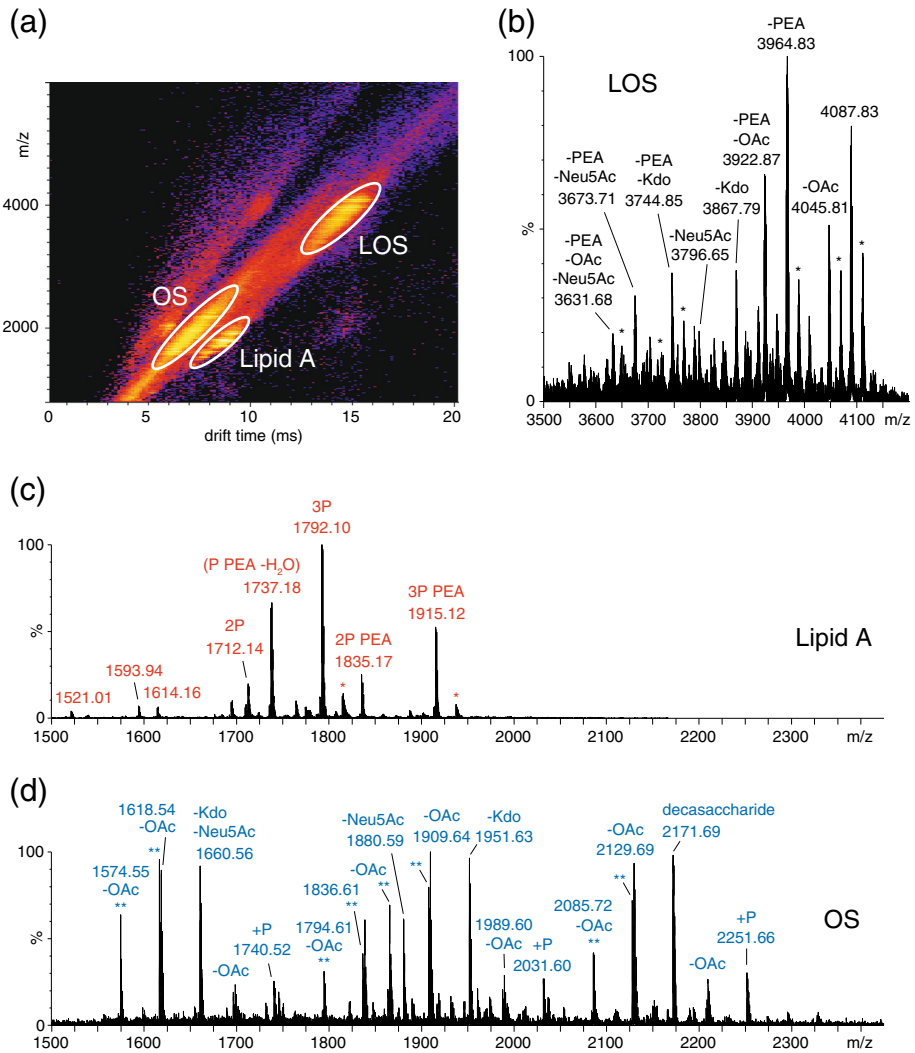

Figure 3. Analysis of the intact LOS from *N. meningitidis* 89I by MALDI-TOF MS with IMS. Panel **(a)** shows a two-dimensional plot of the IMS dataset, and panels **(b)**, **(c)**, and **(d)** show expanded regions of the mass spectra of the $(M–H)^-$ ions, lipid A prompt fragments, and OS prompt fragments, respectively. The lipid A and OS prompt fragments are shown on the same mass range to reveal the clean separation of ions that would otherwise be closely occurring, such as the lipid A fragment ion at *m/z* 1835.17 and the OS fragment ions at *m/z* 1836.61 and 1838.61. Sodiated species are marked with a single asterisk, and decarboxylated oligosaccharide prompt fragments ($–CO_2$, –44 Da) are marked with two asterisks

Glycosidic bond cleavages and cross-ring fragments serve to localize the fatty acid and phosphate substituents on either the reducing or non-reducing terminus of the lipid A structure [53, 54]. In the case of Neisserial lipid A structures, where the distribution of fatty acids is symmetrical on the two glucosamines, the assignment of glycosidic bond fragments can sometimes be ambiguous. For example, it may be possible to assign a given fragment as either a Y-ion or a C-ion, depending on where the charge resides. However, in general, diagnostic ^{0,4}A-type cross-ring fragments are present that unambiguously show which phosphate moieties are present on the non-reducing terminus. In the IMS-MS/MS spectrum shown in Figure 4d, the assignment of *m/z* 986.57 as an ^{0,4}A-ion supports the triphosphorylated structure shown above the spectrum as the major phosphoform. Assignment of the ion at *m/z* 926.54 as a B-ion also fits this phosphoform. However, the ion at *m/z* 944.56 can either be assigned as a C-ion (fitting the depicted phosphoform) or as a Y-ion arising from a phosphoform with a diphosphoryl moiety on the reducing terminus. Minor ions at *m/z* 1006.54 and 1024.51 derive from the corresponding minor species bearing triphosphoryl moieties. Thus, it would appear that under our typical experimental conditions, TWIMS was unable to resolve at least two isobaric lipid A phosphoforms at *m/z* 1792.14, the existence of which was suggested by the IMS-MS/MS analysis. This may be due to the inherent limitations of TWIMS compared with traditional "drift-time" IMS [36], although we have not systematically explored strategies to improve our TWIMS resolution of putative isobaric species of this type.

In similar IMS-MS/MS experiments, oligosaccharide prompt fragments (B-ions) from *N. meningitidis* 89I LOS were selected for CID following IMS separation (Figure 5).

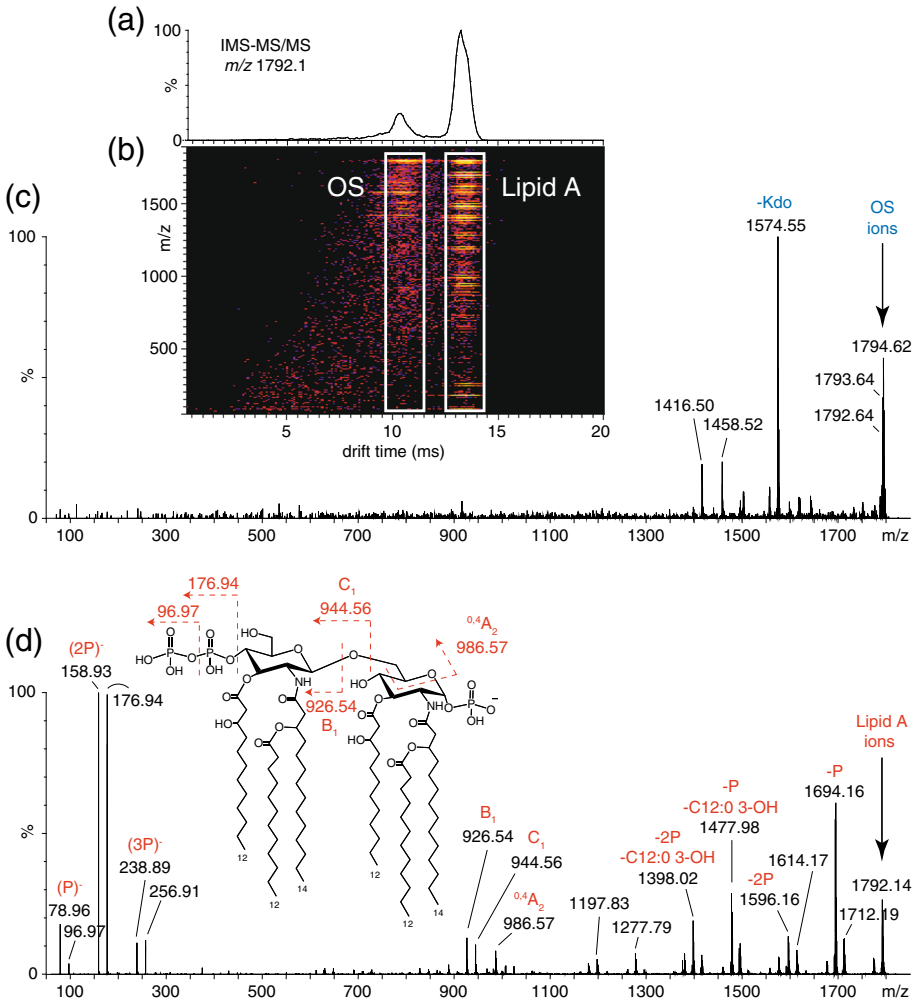

Figure 4. Negative-ion, IMS-MS/MS analysis of the lipid A prompt fragment at *m/z* 1792.1 from *N. meningitidis* 89I LOS. In this experiment, CID was conducted in the Transfer region of the Triwave device after the IMS separation. Panel **(a)** shows the total ion mobilogram above the two-dimensional plot of the IMS-MS/MS data **(b)**. Under the selection conditions employed to achieve high sensitivity, the interfering OS prompt fragment at *m/z* 1794.62 (see Figure 3d) is included in the selection window but is readily resolved by IMS. The OS (*m/z* 1794.62) and lipid A (*m/z* 1792.14) MS/MS spectra were selected from the two-dimensional plot as indicated, and are shown in panels **(c)** and **(d)**, respectively. Major lipid A fragment ions are labeled and shown on the structure inset in panel **(d)**

The resulting negative-ion MS/MS spectrum of the decasaccharide at *m/z* 2171.7 shown in Figure 5b is highly characteristic of results with LOS-derived oligosaccharides from pathogenic *Neisseria*. The fact that the oligosaccharide precursor ions are B-ions to begin with, without free reducing termini, limits reducing terminal decomposition upon CID [55]. The three prominent fragments arise from Y-type cleavages for loss of the branch Kdo (*m/z* 1951.62), the non-reducing terminal Neu5Ac (*m/z* 1880.59), and the concomitant loss of both labile moieties (*m/z* 1660.54). While these abundant fragments readily corroborate the presence of a second Kdo and a Neu5Ac on the oligosaccharide, the negative-ion MS/MS spectra of oligosaccharide prompt fragments containing these moieties usually are lacking in other informative sequence ions.

In an effort to generate additional carbohydrate sequence ions, we have explored MALDI-TOF MS analysis of intact LOS in positive-ion mode, where oligosaccharide prompt fragments are generally much more abundant than lipid A prompt fragments, which may not be detectable at all depending on their phosphorylation states (unpublished findings). When the corresponding positive-ion prompt fragment at *m/z* 2173.7 from *N. meningitidis* 89I LOS was selected for CID following IMS, the MS/MS spectrum shown in Figure 5a was obtained. In addition to high mass fragments corresponding to the Kdo and Neu5Ac losses observed in negative-ion mode, the positive-ion spectrum contains numerous carbohydrate sequence ions, as indicated on the structural inset. Significant peaks for either B- or Y-type or both fragment ion types were observed for seven

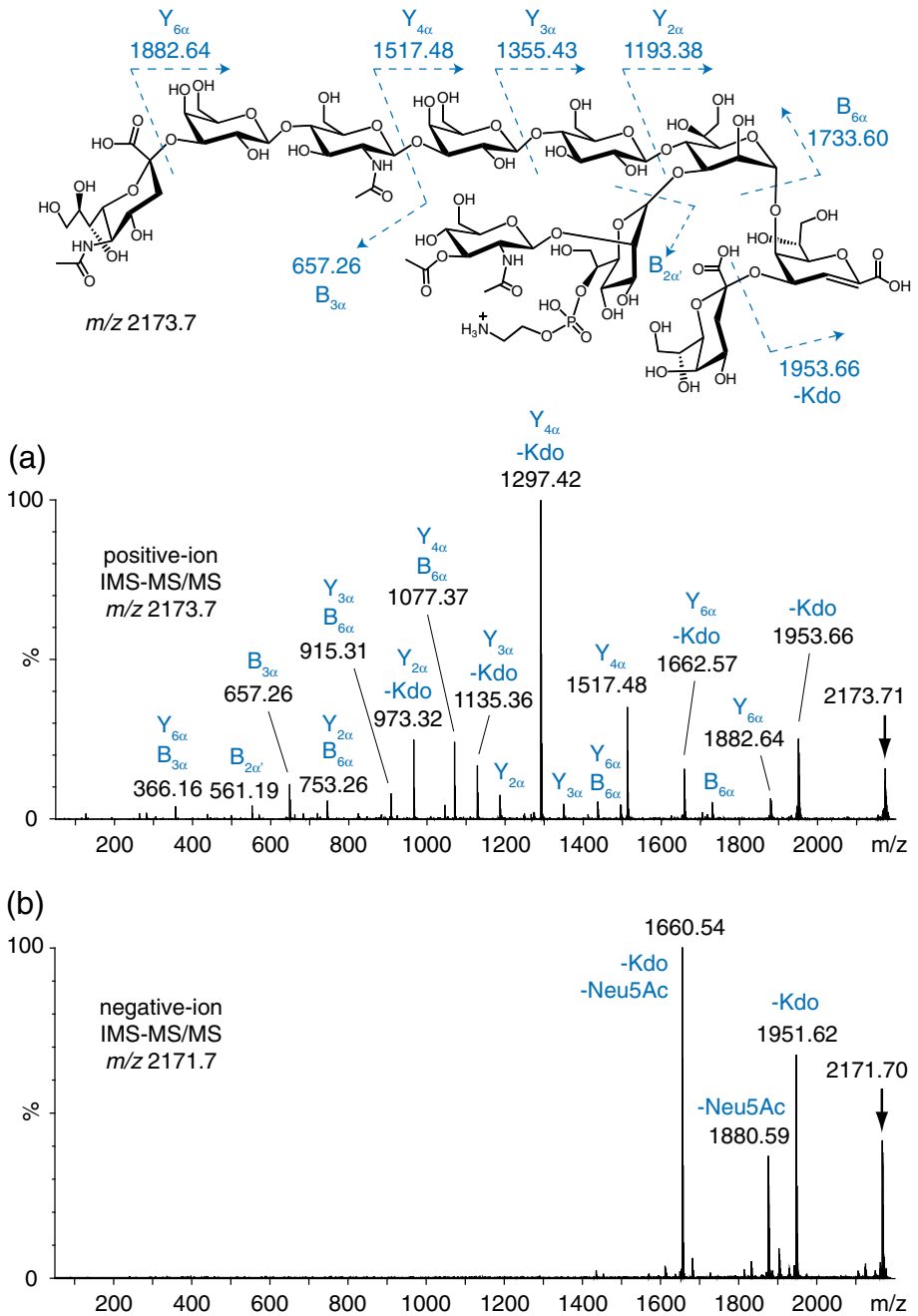

Figure 5. Comparison of positive-ion and negative-ion IMS-MS/MS analysis of the decasaccharide prompt fragment from *N. meningitidis* 89I LOS. CID was conducted in the Transfer region of the Triwave device after the IMS separation. The positive-ion IMS-MS/MS spectrum **(a)** shows a wealth of sequence ions, whereas in the negative-ion mode, the IMS-MS/MS spectrum is dominated by the facile losses of Kdo and Neu5Ac from the OS **(b)**. The structural drawing inset above panel **(a)** shows the positive-ion fragment assignments for this previously characterized Neisserial decasaccharide [42]. Fragment ions arising from two bond cleavages are labeled with notations for both fragmentation mechanisms on the spectrum

of the nine glycosidic bonds in the oligosaccharide. As expected, B-type (*m/z* 657.26) and Y-type (*m/z* 1517.48) ions associated with cleavage to the reducing side of the GlcNAc residue were abundant [45], with the base peak at *m/z* 1297.42 arising from this Y-type cleavage in combination with loss of the branch Kdo. Although significant peaks arising from cross-ring cleavages of the oligosaccharide that can aid in establishing linkage position were not detected, clearly, positive-ion IMS-MS/MS analysis of LOS-derived oligosaccharides produces MS/MS spectra containing a wealth of structural information that aids in assigning compositions and provides some sequence information. As such, the fragmentation patterns of LOS-derived oligosaccharides can be valuable

components of LOS profiling strategies. To establish detailed oligosaccharide compositions, branching patterns, and anomeric assignments for completely unknown oligosaccharide species, other complementary experiments would be required, such as composition analysis, linkage analysis (methylation analysis), MS^n, and 1D and 2D NMR experiments [56].

Analysis of an SR-type LPS from N. flavescens

The thin layer MALDI-TOF MS method is ideal for ionization and detection of intact LOS because of their relatively small size (~3000–6000 Da). The same is true for R-type LPS from organisms such as *E. coli* and *Salmonella* spp. that also lack an *O*-antigen. A number of *Vibrio* spp. [57, 58], as well as some other Gram-negative bacteria such as *Pseudomonas aeruginosa* [59], express SR-type LPS, which contain only one *O*-antigen repeat unit [4]. As noted above, SR-type LPS migrate in the same size range as LOS when analyzed by SDS-PAGE and thus are equally amenable to thin layer MALDI-TOF MS analysis, where specific structural information about both core and *O*-antigen structures can be gleaned.

To investigate the glycoforms of the LPS from *N. flavescens* 4322, we analyzed the intact material by IMS-MS (Figure 6a–d). As shown in Figure 6d, there is clear evidence that the high mass ions in the two clusters

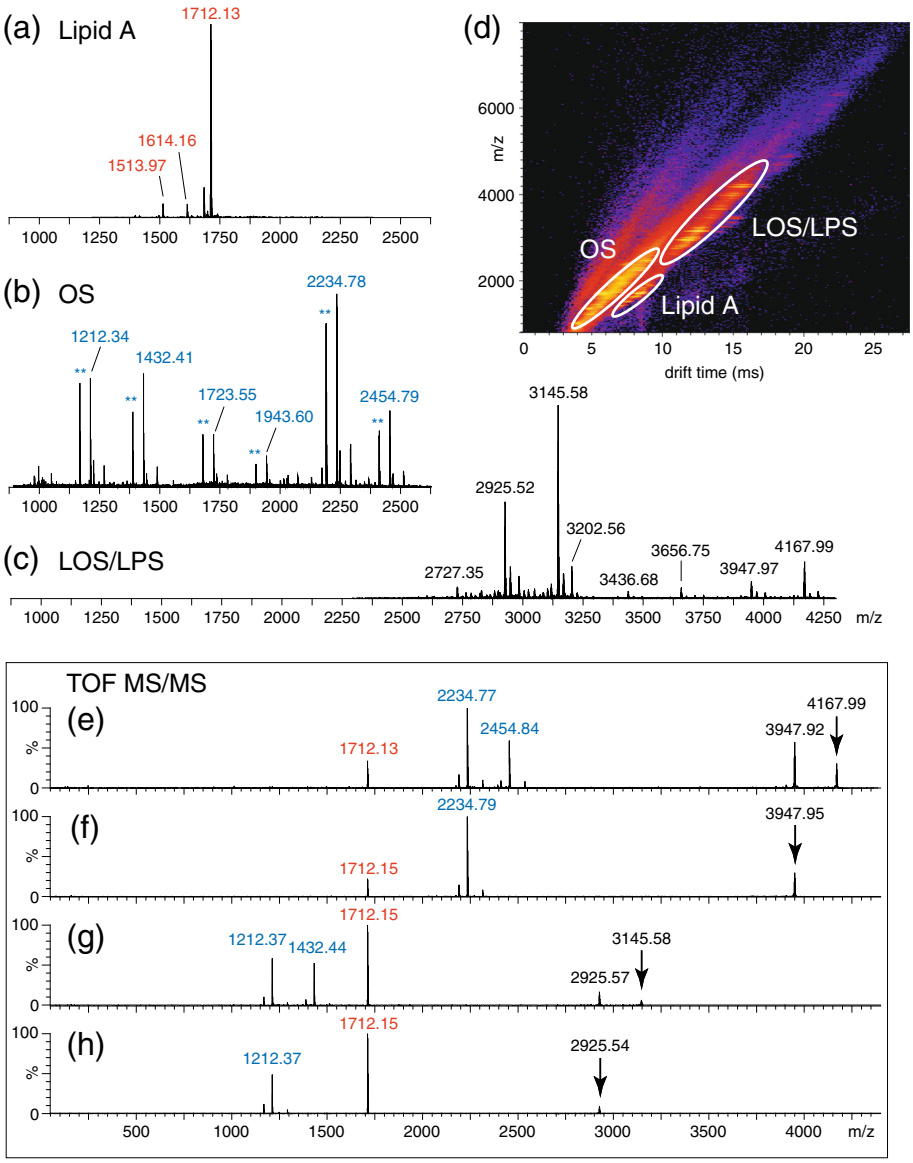

Figure 6. Analysis of the intact LOS from *N. flavescens* 4322 by MALDI-TOF MS with IMS **(a)-(d)**. In the IMS spectrum **(d)**, there is indication of an LPS-like repeat unit in the molecular ion plume. The extracted spectra for the lipid A prompt fragments **(a)**, OS prompt fragments **(b)**, and putative molecular ions **(c)** are shown. Decarboxylated oligosaccharide prompt fragments ($-CO_2$, –44 Da) are marked with two asterisks. To support the molecular ion assignments, TOF-MS/MS spectra were obtained **(e)-(h)** for the four putative molecular ions at *m/z* 4167.99, 3947.95, 3145.58, and 2925.54. All of the precursor ions give the lipid A fragment ion at *m/z* 1712.1 and appropriate corresponding OS fragments, confirming their assignments as intact LOS/LPS species

Table 2. Masses of the Domains of the SR-type LPS from *N. flavescens*

N. flavescens LOS/LPS				
DPLA[a] *m/z*	Core OS *m/z*	Repeat unit *m/z*	Core OS + repeat *m/z*	Intact LOS/LPS $(M–H)^-$
1712.120[b]	*1489.419* [c]	*1022.368*	2511.787	4224.881
1712.120	*1432.412*	*1022.387*	2454.799	4167.970
1712.120	*1269.362*	*1022.398*	2291.760	4004.903
1712.120	*1212.350*	*1022.379*	2234.729	3947.902
1712.120	1489.419			3202.595
1712.120	1432.412			3145.547
1712.120	1269.362			2982.500
1712.120	1212.350			2925.487

[a]Abbreviations used: DPLA = diphosphorylated lipid A; OS = oligosaccharide.
[b]Measured masses (from the spectrum shown in Figure 1c) given in regular font.
[c]Inferred masses of contributing units given in italics.

(*m/z* ~2700–3200 and *m/z* ~3600–4200) are migrating on the same plume, suggesting that they are all LOS/LPS molecular ions. The extracted subspectra (Figure 6a–c) support this interpretation. However, to unequivocally confirm their assignments, all of the putative $(M–H)^-$ ions were individually selected for CID using TOF MS/MS (Figure 6e–h). When selected for CID, the largest species at *m/z* 4167.99 (putative SR-type LPS) readily lost a Kdo residue to give the fragment at *m/z* 3947.92, in addition to an oligosaccharide B-ion at *m/z* 2454.84 and a corresponding lipid A Y-ion at *m/z* 1712.13 that accounted for the full structure. Also present in the spectrum was a smaller oligosaccharide fragment at *m/z* 2234.77, corresponding to the species at *m/z* 2454.84 minus a Kdo residue (Figure 6e). As expected, the MS/MS spectrum of *m/z* 3947.95, already lacking the labile Kdo residue, gave only a single oligosaccharide fragment (*m/z* 2234.79) in addition the lipid A fragment at *m/z* 1712.15 (Figure 6f). Correspondingly, when selected for MS/MS analysis, the two LOS-like species at *m/z* 3145.58 and 2925.54, which also differed by one Kdo residue, showed low mass oligosaccharide fragments at *m/z* 1432.44 and 1212.37, respectively, in addition to the lipid A fragment at *m/z* 1712.15 (Figure 6g and h). From this fragmentation analysis, it was possible to confirm that the mass difference between the high mass and low mass $(M–H)^-$ ions was ~1022.38 Da (see Table 2). Consistent with the minor ions at *m/z* 3656.75 and 3436.68 seen in the $(M–H)^-$ subspectrum (Figure 6c) and the ions at *m/z* 1943.60 and 1723.55 in the oligosaccharide subspectrum (Figure 6b) that represent half of this mass difference, we hypothesize that the ~1022.38 Da moiety represents a hexasaccharide composed of two hexoses (Hex), two deoxyhexoses (dHex), and two *N*-acetylhexosamines (HexNAc) (calculated monoisotopic *m/z* = 1022.3802). MS/MS analyses of the carbohydrate prompt fragments containing this moiety (data not shown) suggest that the repeat unit may in fact be a trisaccharide, HexNAc→Hex→dHex, repeated twice in the SR-type LPS. Although they usually contain only one repeat unit, SR-type LPS may contain two *O*-antigen subunits where the reducing termini of the subunits have different anomeric configurations [60]. A dHex moiety, rhamnose, was recently reported as a constituent of the LPS of another commensal species of *Neisseria*, *N. sicca* [61]. Further detailed analyses of the LOS/LPS from *N. flavescens* 4322 are required in order to identify monosaccharide constituents and confirm the proposed composition of the *O*-antigen.

Conclusions

We have shown that intact LOS and SR-type LPS are ideally suited to be studied by IMS-MS and IMS-MS/MS, particularly when ionized by MALDI MS in the negative-ion mode. The propensity for intact LOS to form in-source prompt fragments from cleavage between the two domains of the molecule generates an informative ensemble of singly charged ions that are readily separated according to chemical class by IMS. More accurate and detailed information about LOS architecture can be obtained when clean subspectra of oligosaccharide and lipid A prompt fragments are extracted during MS analysis. Importantly, our results demonstrate that by simultaneously profiling all domains of the molecules in IMS mode, we enhanced our ability to "fingerprint" intact LOS and assign compositions to an ensemble of structures produced by a given bacterial strain. We have tested the approach with a few other Gram-negative organisms that produce LOS ranging up to about 5500 Da, such as *Campylobacter* and *Vibrio* spp., and have achieved comparable results to those presented here for Neisserial LOS.

Furthermore, we have shown that selection of LOS prompt fragments for MS/MS analysis (pseudo-MS^3 analysis) following IMS separation generates cleaner MS/MS spectra compared with those obtained without IMS. Due to the excellent separation of oligosaccharide and lipid A species on different ion plumes, precursor ion windows for IMS-MS/MS can be set to maximize sensitivity. These methods facilitate identification of biologically important LOS substituents including phosphate and PEA moieties on the lipid A and oligosaccharide, as well as acetate and Neu5Ac on the oligosaccharide domain.

We have shown that diagnostic fragmentation of the lipid A species can serve to localize fatty acids and phosphate moieties to either the reducing or non-reducing terminal GlcN, whereas fragmentation of the LOS-derived carbohydrate moieties is useful to establish generic monosaccharide compositions, identify biologically important moieties, and provide limited sequence information.

As information on the molecular determinants of LOS bioactivity continues to emerge, particularly with regard to the role of lipid A phosphorylation states in inflammatory signaling [11] and immune tolerance [62], the need to decipher LOS heterogeneity becomes more urgent. Moreover, LOS and LPS structural variation could underlie some distinctions between commensal and pathogenic Gram-negative bacteria [12]. Our results indicate that the profiling and analysis of intact LOS by high-resolution, MALDI-TOF MS coupled with IMS should be a valuable addition to the variety of methods used to investigate these bioactive glycolipids.

Acknowledgments

This work was supported by Merit Review Award BX000727 from the Research Service of the U.S. Department of Veterans Affairs (G.A.J.). The authors also acknowledge NIH/National Center for Research Resources Shared Instrumentation Grant S10 RR029446 (H. E. Witkowska) for acquisition of the Synapt G2 HDMS, which is located in the University of California, San Francisco's Sandler-Moore Mass Spectrometry Core Facility (supported by the Sandler Family Foundation, the Gordon and Betty Moore Foundation, NIH/NCI Cancer Center Support Grant P30 CA082103, and the Canary Foundation). G.A.J. is the recipient of a Senior Research Career Scientist Award from the Veterans Affairs Medical Research Service. This is paper number 115 from the Center for Immunochemistry.

References

1. Alexander, C., Rietschel, E.T.: Bacterial lipopolysaccharides and innate immunity. J. Endotoxin Res. **7**, 167–202 (2001)
2. Rietschel, E.T., Brade, L., Schade, U., Seydel, U., Zähringer, U., Brandenburg, K., Helander, I., Holst, O., Kondo, S., Kuhn, H.M., Lindner, B., Röhrscheidt, E., Russa, R., Labischinski, H., Naumann, D., Brade, H.: Bacterial lipopolysaccharides: relationship of structure and conformation to endotoxic activity, serological specificity, and biological function. Adv. Exp. Med. Biol. **256**, 81–99 (1990)
3. Griffiss, J.M., Schneider, H.: The chemistry and biology of lipooligosaccharides: the endotoxins of bacteria of the respiratory and genital mucosae. In: Brade, H., Opal, S.M., Vogel, S.N., Morrison, D.C. (eds.) Endotoxin in Health and Disease, pp. 179–194. Marcel Dekker, Inc., New York (1999)
4. Caroff, M., Karibian, D.: Structure of bacterial lipopolysaccharides. Carbohydr. Res. **338**, 2431–2447 (2003)
5. Gnauck, A., Lentle, R.G., Kruger, M.C.: The characteristics and function of bacterial lipopolysaccharides and their endotoxic potential in humans. Int. Rev. Immunol. (2015). doi:10.3109/08830185.2015.1087518
6. Brouwer, M.C., Spanjaard, L., Prins, J.M., van der Ley, P., van de Beek, D., van der Ende, A.: Association of chronic meningococcemia with infection by meningococci with underacylated lipopolysaccharide. J. Infect. **62**, 479–483 (2011)
7. Zhou, X., Gao, X., Broglie, P.M., Kebaier, C., Anderson, J.E., Thom, N., Apicella, M.A., Sempowski, G.D., Duncan, J.A.: Hexa-acylated lipid A is required for host inflammatory response to *Neisseria gonorrhoeae* in experimental gonorrhea. Infect. Immun. **82**, 184–192 (2014)
8. Lewis, L.A., Shafer, W.M., Dutta Ray, T., Ram, S., Rice, P.A.: Phosphoethanolamine residues on the lipid A moiety of *Neisseria gonorrhoeae* lipooligosaccharide modulate binding of complement inhibitors and resistance to complement killing. Infect. Immun. **81**, 33–42 (2013)
9. John, C.M., Liu, M.F., Jarvis, G.A.: Natural phosphoryl and acyl variants of lipid A from *Neisseria meningitidis* strain 89I differentially induce tumor necrosis factor-α in human monocytes. J. Biol. Chem. **284**, 21515–21525 (2009)
10. John, C.M., Liu, M.F., Jarvis, G.A.: Profiles of structural heterogeneity in native lipooligosaccharides of *Neisseria* and cytokine induction. J. Lipid Res. **50**, 424–438 (2009)
11. Liu, M., John, C.M., Jarvis, G.A.: Phosphoryl moieties of lipid A from *Neisseria meningitidis* and *N. gonorrhoeae* lipooligosaccharides play an important role in activation of both MyD88- and TRIF-dependent TLR4-MD-2 signaling pathways. J. Immunol. **185**, 6974–6984 (2010)
12. John, C.M., Liu, M., Phillips, N.J., Yang, Z., Funk, C.R., Zimmerman, L.I., Griffiss, J.M., Stein, D.C., Jarvis, G.A.: Lack of lipid A pyrophosphorylation and functional *lptA* reduces inflammation by *Neisseria* commensals. Infect. Immun. **80**, 4014–4026 (2012)
13. John, C.M., Phillips, N.J., Din, R., Liu, M., Rosenqvist, E., Høiby, E.A., Stein, D.C., Jarvis, G.A.: Lipooligosaccharide structures of invasive and carrier isolates of *Neisseria meningitidis* are correlated with pathogenicity and carriage. J. Biol. Chem. **291**, 3224–3238 (2016)
14. Coats, S.R., Berezow, A.B., To, T.T., Jain, S., Bainbridge, B.W., Banani, K.P., Darveau, R.P.: The lipid A phosphate position determines differential host Toll-like receptor 4 responses to phylogenetically related symbiotic and pathogenic bacteria. Infect. Immun. **79**, 203–210 (2011)
15. Porat, N., Apicella, M.A., Blake, M.S.: *Neisseria gonorrhoeae* utilizes and enhances the biosynthesis of the asialoglycoprotein receptor expressed on the surface of the hepatic HepG2 cell line. Infect. Immun. **63**, 1498–1506 (1995)
16. Day, C.J., Tran, E.N., Semchenko, E.A., Tram, G., Hartley-Tassell, L.E., Ng, P.S., King, R.M., Ulanovsky, R., McAtamney, S., Apicella, M.A., Tiralongo, J., Morona, R., Korolik, V., Jennings, M.P.: Glycan:glycan interactions: high affinity biomolecular interactions that can mediate binding of pathogenic bacteria to host cells. Proc. Natl. Acad. Sci. U. S. A. **112**, E7266–E7275 (2015)
17. Harvey, H.A., Swords, W.E., Apicella, M.A.: The mimicry of human glycolipids and glycosphingolipids by the lipooligosaccharides of pathogenic *Neisseria* and *Haemophilus*. J. Autoimmun. **16**, 257–262 (2001)
18. Moran, A.P., Prendergast, M.M., Appelmelk, B.J.: Molecular mimicry of host structures by bacterial lipopolysaccharides and its contribution to disease. FEMS Immunol. Med. Microbiol. **16**, 105–115 (1996)
19. Schneider, H., Griffiss, J.M., Boslego, J.W., Hitchcock, P.J., Zahos, K.M., Apicella, M.A.: Expression of paragloboside-like lipooligosaccharides may be a necessary component of gonococcal pathogenesis in men. J. Exp. Med. **174**, 1601–1605 (1991)
20. Cheng, H., Yang, Z., Estabrook, M.M., John, C.M., Jarvis, G.A., McLaughlin, S., Griffiss, J.M.: Human lipooligosaccharide IGG that prevents endemic meningococcal disease recognizes an internal lacto-*N*-neotetraose structure. J. Biol. Chem. **286**, 43622–43633 (2011)
21. Estabrook, M.M., Jarvis, G.A., McLeod Griffiss, J.: Affinity-purified human immunoglobulin G that binds a lacto-*N*-neotetraose-dependent lipooligosaccharide structure is bactericidal for serogroup B *Neisseria meningitidis*. Infect. Immun. **75**, 1025–1033 (2007)
22. Lewis, L.A., Carter, M., Ram, S.: The relative roles of factor H binding protein, Neisserial surface protein A, and lipooligosaccharide sialylation in regulation of the alternative pathway of complement on meningococci. J. Immunol. **188**, 506–5072 (2012)
23. Ram, S., Cox, A.D., Wright, J.C., Vogel, U., Getzlaff, S., Boden, R., Li, J., Plested, J.S., Meri, S., Gulati, S., Stein, D.C., Richards, J.C., Moxon, E.R., Rice, P.A.: Neisserial lipooligosaccharide is a target for complement component C4b. Inner core phosphoethanolamine residues define C4b linkage specificity. J. Biol. Chem. **278**, 50853–50862 (2003)
24. Banoub, J.H., El Aneed, A., Cohen, A.M., Joly, N.: Structural investigation of bacterial lipopolysaccharides by mass spectrometry and tandem mass spectrometry. Mass Spectrom. Rev. **29**, 606–650 (2010)
25. Hashii, N., Isshiki, Y., Iguchi, T., Kondo, S.: Structural analysis of the carbohydrate backbone of *Vibrio parahaemolyticus* O2 lipopolysaccharides. Carbohydr. Res. **338**, 1063–1071 (2003)

26. Vinogradov, E., Korenevsky, A., Beveridge, T.J.: The structure of the carbohydrate backbone of the LPS from *Shewanella putrefaciens* CN32. Carbohydr. Res. **337**, 1285–1289 (2002)
27. Li, J., Bauer, S.H., Mansson, M., Moxon, E.R., Richards, J.C., Schweda, E.K.: Glycine is a common substituent of the inner core in *Haemophilus influenzae* lipopolysaccharide. Glycobiology **11**, 1009–1015 (2001)
28. Dzieciatkowska, M., Brochu, D., van Belkum, A., Heikema, A.P., Yuki, N., Houliston, R.S., Richards, J.C., Gilbert, M., Li, J.: Mass spectrometric analysis of intact lipooligosaccharide: direct evidence for *O*-acetylated sialic acids and discovery of *O*-linked glycine expressed by *Campylobacter jejuni*. Biochemistry **46**, 14704–14714 (2007)
29. O'Brien, J.P., Needham, B.D., Brown, D.B., Trent, M.S., Brodbelt, J.S.: Top-down strategies for the structural elucidation of intact Gram-negative bacterial endotoxins. Chem. Sci. **5**, 4291–4301 (2014)
30. Kilar, A., Dornyei, A., Kocsis, B.: Structural characterization of bacterial lipopolysaccharides with mass spectrometry and on- and off-line separation techniques. Mass Spectrom. Rev. **32**, 90–117 (2013)
31. Sturiale, L., Garozzo, D., Silipo, A., Lanzetta, R., Parrilli, M., Molinaro, A.: New conditions for matrix-assisted laser desorption/ionization mass spectrometry of native bacterial R-type lipopolysaccharides. Rapid Commun. Mass Spectrom. **19**, 1829–1834 (2005)
32. Stephenson, H.N., John, C.M., Naz, N., Gundogdu, O., Dorrell, N., Wren, B.W., Jarvis, G.A., Bajaj-Elliott, M.: *Campylobacter jejuni* lipooligosaccharide sialylation, phosphorylation, and amide/ester linkage modifications fine-tune human Toll-like receptor 4 activation. J. Biol. Chem. **288**, 19661–19672 (2013)
33. de Hoffmann, E., Stroobant, V.: Mass Spectrometry: Principles and Applications, 3rd edn. John Wiley and Sons, Ltd., West Sussex (2007)
34. Gibson, B.W., Engstrom, J.J., John, C.M., Hines, W., Falick, A.M.: Characterization of bacterial lipooligosaccharides by delayed extraction matrix-assisted laser desorption ionization time-of-flight mass spectrometry. J. Am. Soc. Mass Spectrom. **8**, 645–658 (1997)
35. Sturiale, L., Palmigiano, A., Silipo, A., Knirel, Y.A., Anisimov, A.P., Lanzetta, R., Parrilli, M., Molinaro, A., Garozzo, D.: Reflectron MALDI TOF and MALDI TOF/TOF mass spectrometry reveal novel structural details of native lipooligosaccharides. J. Mass Spectrom. **46**, 1135–1142 (2011)
36. Kanu, A.B., Dwivedi, P., Tam, M., Matz, L., Hill Jr., H.H.: Ion mobility-mass spectrometry. J. Mass Spectrom. **43**, 1–22 (2008)
37. Pringle, S.D., Giles, K., Wildgoose, J.L., Williams, J.P., Slade, S.E., Thalassinos, K., Bateman, R.H., Bowers, M.T., Scrivens, J.H.: An investigation of the mobility separation of some peptide and protein ions using a new hybrid quadrupole/travelling wave IMS/oa-ToF instrument. Int. J. Mass Spectrom. **261**, 1–12 (2007)
38. Giles, K., Pringle, S.D., Worthington, K.R., Little, D., Wildgoose, J.L., Bateman, R.H.: Applications of a traveling wave-based radio-frequency-only stacked ring ion guide. Rapid Commun. Mass Spectrom. **18**, 2401–2414 (2004)
39. Fenn, L.S., McLean, J.A.: Biomolecular structural separations by ion mobility-mass spectrometry. Anal. Bioanal. Chem. **391**, 905–909 (2008)
40. Fenn, L.S., Kliman, M., Mahsut, A., Zhao, S.R., McLean, J.A.: Characterizing ion mobility-mass spectrometry conformation space for the analysis of complex biological samples. Anal. Bioanal. Chem. **394**, 235–244 (2009)
41. Kliman, M., May, J.C., McLean, J.A.: Lipid analysis and lipidomics by structurally selective ion mobility-mass spectrometry. Biochim. Biophys. Acta **1811**, 935–945 (2011)
42. Kogan, G., Uhrin, D., Brisson, J.R., Jennings, H.J.: Structural basis of the *Neisseria meningitidis* immunotypes including the L4 and L7 immunotypes. Carbohydr. Res. **298**, 191–199 (1997)
43. Apicella, M.A., Griffiss, J.M., Schneider, H.: Isolation and characterization of lipopolysaccharides, lipooligosaccharides, and lipid A. Methods Enzymol. **235**, 242–252 (1994)
44. Westphal, O., Jann, K.: Bacterial lipopolysaccharides. Extraction with Phenol-Water and Further Applications of the Procedure. In: Methods in Carbohydrate Chemistry. Whistler, R.L. (Ed.) Academic Press: New York, NY pp. 83–91 (1965)
45. Domon, B., Costello, C.E.: A systematic nomenclature for carbohydrate fragmentations in FAB-MS/MS spectra of glycoconjugates. Glycoconj. J. **5**, 397–409 (1988)
46. Tsai, C.M., Chen, W.H., Balakonis, P.A.: Characterization of terminal NeuNAcα2-3Galβ1-4GlcNAc sequence in lipooligosaccharides of *Neisseria meningitidis*. Glycobiology **8**, 359–365 (1998)
47. Tsai, C.M., Jankowska-Stephens, E., Mizanur, R.M., Cipollo, J.F.: The fine structure of *Neisseria meningitidis* lipooligosaccharide from the M986 strain and three of its variants. J. Biol. Chem. **284**, 4616–4625 (2009)
48. Wakarchuk, W.W., Gilbert, M., Martin, A., Wu, Y., Brisson, J.R., Thibault, P., Richards, J.C.: Structure of an α-2,6-sialylated lipooligosaccharide from *Neisseria meningitidis* immunotype L1. Eur. J. Biochem. **254**, 626–633 (1998)
49. Tsang, R.S., Law, D.K., Tsai, C., Ng, L.: Detection of the lst gene in different serogroups and LOS immunotypes of *Neisseria meningitidis*. FEMS Microbiol. Lett. **199**, 203–206 (2001)
50. Kulshin, V.A., Zahringer, U., Lindner, B., Frasch, C.E., Tsai, C.M., Dmitriev, B.A., Rietschel, E.T.: Structural characterization of the lipid A component of pathogenic *Neisseria meningitidis*. J. Bacteriol. **174**, 1793–1800 (1992)
51. Shin, J.E.N., Ackloo, S., Mainkar, A.S., Monteiro, M.A., Pang, H., Penner, J.L., Aspinall, G.O.: Lipo-oligosaccharides of *Campylobacter jejuni* serotype O:10. Structures of core oligosaccharide regions from a bacterial isolate from a patient with the Miller-Fisher syndrome and from the serotype reference strain. Carbohydr. Res. **305**, 223–232 (1997)
52. Jones, J.W., Shaffer, S.A., Ernst, R.K., Goodlett, D.R., Turecek, F.: Determination of pyrophosphorylated forms of lipid A in Gram-negative bacteria using a multivaried mass spectrometric approach. Proc. Natl. Acad. Sci. U. S. A. **105**, 12742–12747 (2008)
53. Phillips, N.J., Adin, D.M., Stabb, E.V., McFall-Ngai, M.J., Apicella, M.A., Gibson, B.W.: The lipid A from *Vibrio fischeri* lipopolysaccharide: a unique structure bearing a phosphoglycerol moiety. J. Biol. Chem. **286**, 21203–21219 (2011)
54. Schilling, B., McLendon, M.K., Phillips, N.J., Apicella, M.A., Gibson, B.W.: Characterization of lipid A acylation patterns in *Francisella tularensis*, *Francisella novicida*, and *Francisella philomiragia* using multiple-stage mass spectrometry and matrix-assisted laser desorption/ionization on an intermediate vacuum source linear ion trap. Anal. Chem. **79**, 1034–1042 (2007)
55. Dallinga, J.W., Heerma, W.: Reaction mechanism and fragment ion structure determination of deprotonated small oligosaccharides, studied by negative ion fast atom bombardment (tandem) mass spectrometry. Biol. Mass Spectrom. **20**, 215–231 (1991)
56. Mulloy, B., Hart, G.W., Stanley, P.: Structural analysis of glycans. In: Varki, A., Cummings, R.D., Esko, J.D., Freeze, H.H., Stanley, P., Bertozzi, C.R., Hart, G.W., Etzler, M.E. (eds.) Essentials of Glycobiology, 2nd edn, pp. 661–678. Cold Spring Harbor Laboratory Press, Cold Spring Harbor (2009)
57. Nakhamchik, A., Wilde, C., Rowe-Magnus, D.A.: Identification of a Wzy polymerase required for group IV capsular polysaccharide and lipopolysaccharide biosynthesis in *Vibrio vulnificus*. Infect. Immun. **75**, 5550–5558 (2007)
58. Post, D.M., Yu, L., Krasity, B.C., Choudhury, B., Mandel, M.J., Brennan, C.A., Ruby, E.G., McFall-Ngai, M.J., Gibson, B.W., Apicella, M.A.: *O*-antigen and core carbohydrate of *Vibrio fischeri* lipopolysaccharide: composition and analysis of their role in *Euprymna scolopes* light organ colonization. J. Biol. Chem. **287**, 8515–8530 (2012)
59. Bystrova, O.V., Knirel, Y.A., Lindner, B., Kocharova, N.A., Kondakova, A.N., Zähringer, U., Pier, G.B.: Structures of the core oligosaccharide and O-units in the R- and SR-type lipopolysaccharides of reference strains of *Pseudomonas aeruginosa* O-serogroups. FEMS Immunol. Med. Microbiol. **46**, 85–99 (2006)
60. Vinogradov, E., Caroff, M.: Structure of the *Bordetella trematum* LPS O-chain subunit. FEBS Lett. **579**, 18–24 (2005)
61. O'Connor, E.T., Zhou, H., Bullock, K., Swanson, K.V., Griffiss, J.M., Reinhold, V.N., Miller, C.J., Stein, D.C.: Structural characterization of an oligosaccharide made by *Neisseria sicca*. J. Bacteriol. **191**, 3311–3320 (2009)
62. Liu, M., John, C.M., Jarvis, G.A.: Induction of endotoxin tolerance by pathogenic *Neisseria* is correlated with the inflammatory potential of lipooligosaccharides and regulated by microRNA-146a. J. Immunol. **192**, 1768–1777 (2014)